Design of prototype dual axis tracker solar panel controlled by geared dc servo motors

A. Mansouri[*], F. Krim, Z. Khouni
Laboratory of Power Electronics and Industrial Control (LEPCI)
Department of Electronics, Faculty of Technology,
University Ferhat Abbas of SETIF1
El Maabouda, Route de Béjaia, Sétif 19000, Algeria

Abstract:

Sunlight sensing for maximum illumination, providing initial position and delays of PV panel, design of an adequate control unit for minimal consuming servo motors are the main challenges of solar tracking systems. That is the objective of this paper to design and implement an automatic control for directing maximum solar illumination to a photovoltaic (PV) panel. The proposed prototype dual axis solar tracker panel is used to optimize the conversion of solar energy into electricity by orienting the panel toward the real position of the sun, at a cost of mechanical complexity and maintenance need, for the best efficiency. In hardware development, two geared DC servo motors are pulse width modulation (PWM) controlled by a drive unit moving the panel using four light dependant resistors (LDR) to provide analog signals processed by a simple and low energy ATMEGA328P microcontroller with Arduino. For the software part, after data processing, a C++ programming controls two DC servo motors to position light sensors in the most favorable direction, where solar panel and sensors will be perpendicular to the sunlight.

[*] A. Mansouri. Tel.:+213 36 61 60 63.
E-mail address: mansouri51@yahoo.com

Keywords: Arduino uno; dual axis; light dependant resistor; low cost solar tracker PWM control

1. Introduction

Regarding continuous depletion and pollution by using fossil fuels (oil, natural gas, coal...), thermonuclear (Uranium, plutonium...) and the increasing demand for energy during last forty years, researchers over the world try to develop new technologies to produce clean electrical renewable energy (REn) sources, so as solar and wind energy, considered as inexhaustible resources. Solar rays produced everyday to our planet is equivalent to million times consumption of the humanity global electrical need of energy. Solar energy is abundant, non-polluting, silent, reliable, free, and inexhaustible, need very low maintenance. For this reason, solar energy will be the most used to produce clean electricity.

Solar trackers are devices that orient solar panels, Fresnel reflector, mirrors or lenses towards the sun to receive maximum radiation as light and heat to be converted to thermal energy or to produce electricity. In 1839, the French physicist Alexandre-Edmond Becquerel was the first researcher who discovers that sunlight could be transformed into electricity. It is the photovoltaic (PV) effect. One century later, the first PV cells where constructed. The early solar modules were used in space in 1958. Other emerging technologies using multi-junction cells are concentrator photovoltaic (CPV) and concentrated solar power (CSP) which must use trackers to be pointed at the sun unless no energy will be produced. For these reasons, researchers are interested to motorize solar trackers. Mechanical and electrical are the main types of sun trackers. In 1962, Finster introduced the first purely mechanical tracker [1]. In 1963, Saavedra designed an automatic electronic control mechanism [2]. After that, several works have been carried out on the design of single and dual solar tracking systems using electromechanical actuators to allow about 30% to 60% more produced energy than fixed system because sunlight remains perpendicular to the PV panels [3-8]. Then, for improving the efficiency of PV conversion, we can use single or dual axis solar tracking [9-18], the optimization of solar cell configuration and geometry, new materials and technologies for optoelectronic applications etc...[19-22]. Although, solar trackers can gain more energy, some problems appear in their installation such as energy consumption, cost, reliability and maintenance. It is not recommended to use solar tracker for small panels because of high energy losses in the driving systems. We show that very low power consumption is *2* to *3%* of the increased energy by tracking device.

The strategic choice of Algeria, a country of Northern Africa on the Mediterranean coast which ranges in latitude from *18.96* to *37.09* north and in longitude from *8.69* west to *11.95* east, is motivated by one of the most important potential solar for renewable energy in the world, recovered from sunlight reaching *3900 h*, particularly in the Sahara desert. A solar radiation Algerian map demonstrates solar energy potentials of specific zone to provide useful information for optimum plant selection of solar energy system [23]. This map can be used as database for future investments in solar energy showing that the highest intensity is around the area of Djanet (southern Algerian desert) and the less intense area is around Ksar Chellala (Tiaret High Planes).

In 2007, the first hybrid plant in the world constructed is located in Hassi R'Mel in southern Algerian desert. It is an ISCC (Integrated Solar Combined Cycle) composed of a conventional combined cycle and a solar field with a nominal thermal power of *150* MW. The goal of this project was to integrate the solar thermal technology in a conventional power plant which integrate a solar field of CCP (parabolic through collector) covering a reflective area of $180\ 000\ m^2$. This combined use, reduces the cost and facilitates the deployment of renewable energies in new industrializing countries. The power plant will be constructed in Boughezoul, on the northern edge of the Sahara desert (Aures), and will serve primarily as a pilot and research facility. It will be able to operate using just solar energy or as hybrid power plant fuelled by a combination of solar power and gas.

Algeria is engaged in a new age of sustainable energy use [24]. The program consists of installing up to *22 GW* of power generating capacity from renewable sources between *2011* and *2030*, of which *12 GW* will be intended to meet the domestic electricity demand and *10 GW* destined for export. This last option depends on the availability of a demand that is ensured on the long term by reliable partners as well as on attractive external funding. It is expected that about *40%* of electricity produced for domestic consumption will be from renewable energy sources by *2030*. This document was produced by the Ministry of Energy and Mines. Designed and printed by SATINFO, Sonelgaz Group Company.

In this context, this paper involves design and control of the prototype of a dual axis solar tracking system for solar PV panel to improve energy efficiency. Tracking system for solar PV panel improves extraction of maximum solar energy. The system is composed of two basic parts, the mechanical assembly and the electrical parts design. The electric part is composed of four identical LDR as the input, the ATMEGA microcontroller as the controller and two servo motors form the output.

2. Solar Tracker Panels

Taking into account geographic situation in Africa, Algeria disposes one of the most important sunny capacities in the world with $2200\ KWh/m^2/annum$. The insolation on the most areas of the annual national territories reaches *2000* hours and could reach *3900* hours in the Sahara. Daily received energy on a horizontal area of $1m^2$ is nearly *5*

KWh on the major zones, *1700 KWh/m*^{2}*/annum* on the northern side and *2263 KWh/m*^{2}*/annum* on the southern side of the country [24-27]. Sunny capacities exceed *5000 TWh*. Table 1 shows the solar potential in three principal zones (coast zone, high planes, sahara) of Algerian territory.

Solar trackers represented in Fig. 1 are a field of PV panels mounted on a moving surface following the trajectory of the sun using dual axis trackers. Using a single axis, the panels could be installed in an inclined plan with a fixed angle on vertical pylon which will orient the PV field in the direction of the sun along the sunny day. The single axis panel could be as well on the same plan of the inclined panels which will be tipping from east to west in the direction of the sun. Dual axis solar tracker is mechanically more complex leaving the plan of the PV panels always in the perpendicular direction to the sun for any position in the sky.

The basic specifications which differentiate the trackers compared to stationary ones are the electrical production gain, orientation mono or multi axial, robustness (against wind) and reliability, and cost.

Using a dual axis solar tracker, the PV modules produces up to *40 %* of energy per annum with difference of production more significant (>*5times*) in higher consuming electrical energy hours at a cost of mechanical complexity and maintenance need [5].

3. Moving PV Panels Interest

Two basic most used solar PV panels are the single axis and dual axis trackers. Single axis tracker can either have a horizontal or a vertical axis. The dual axis solar PV panel tracker is characterized by the capability to move in both horizontal and vertical directions. The vertical and horizontal motion of the panel is obtained by taking altitude angle and azimuth angle as reference making them able to track the sun apparent motion anywhere in the world throughout the day at any seasons. Furthermore, during seasonal changes, latitudinal sun offset must be compensated.

During the day, the sun is moving continuously; contrary to the fixed position PV generator that loses an enormous quantity of energy. To optimise the efficiency, the panels will be installed in the Algerian south area (Sahara). The energy collected by PV panels is maximal only at mi day as seen in Fig. 2. For this reason, if the PV panels are continuously oriented towards the sun, the maximal power will be provided for a long period of the day.

During a sunny day, *one kWp* system well oriented provides *5.5 kWh* of energy. The same tracker system, in the same sunny conditions, provides *11 kWh*. Fig. 2 illustrates comparison of their production [5].

4. Methodology and technique of PV Panels

This project consists on designing a dual axis tracker solar panel prototype, controlled by geared dc servo motors and analysing its working. It is composed of three main parts which are four LDR forming the inputs, the Arduino Uno as the ATMEGA328P microcontroller and two servo motors as the outputs where the block diagram is represented in Fig. 3. Analog signals from the cadmium sulfide LDR are captured by the ATMEGA328P converted to digital signals by Analog/Digital converters, adjusted by two potentiometers (R_{TOL}, R_{VIT}) and sent to two PWM controlled servo motors to move panel towards the sun rays.

Fig. 4 shows LM 7805 positive voltage regulator providing *+5V* required by the microcontroller and most of components of our realization.

The system is designed in two basic parts, the mechanical and the electrical.

4.1 Different components of the electric design

In this section, we are basically interested to components of the solar tracker to orient panel towards solar rays. The components of the hardware design are four LDR, the Arduino Uno microcontroller and two servo motors.

4.1.1 Light Dependant Resistor

Light dependant resistor (LDR) or Cds photocell shown in Fig. 5-a composed of a high resistivity semiconductor, is a component whose resistor value decreases exponentially when the sunlight intensity (illumination in *lux*) increases as shown in Fig. 5-b. This intensity of light sensed by the LDR is used as analog input voltage to the ATMEGA microcontroller.

For our application, we use four identical LDR in a lunette disposed in cross on the panel surface and optically isolated by an opaque plate as shown in Fig. 5-c, so that their illumination are similar only if the lunette is pointed toward the sun.

This lunette is fixed on PV panel and placed on the same plan. These form a sensor designed to detect the sun position. A signal error is generated if the system is none pointed. It is the signal which will be used by the microcontroller to deliver the adequate control to DC servo motors. To process this signal, we have used a voltage divider for each LDR.

The output voltage *Vout* is proportional to the light intensity. *Vout* will increase when the maximum light is captured by the LDR and *Vout* is weak when the LDR is in the shadow, expressed by:

$$V_{out} = \frac{V_{in}.R}{(R + R_{LDR})} \tag{1}$$

4.1.2 Servo motors

The objective of servo motors is to provide an exact movement as a response to an external control. It is an actuator mixing electronic, mechanic and automatic. Servo motors high torque servo having very large power range, are available in a wide variety of frame sizes from small to large, capable of running huge machines, have an excellent power to weight size ratio given their best efficiency (*80-90%*), will do fine with low speed applications given low friction and the correct gear ratio leading to a very low heat production, vibration and very little noise.

The servo motor in Fig. 6 is an assembly of three basic blocks, a body comprising all the mechanics and the electronics, a cable to lead power and the control (reference signal), a pioneer attached to the servo motor axis. We attach on the pioneer the mechanic parts to move (arm, wheel...).

This type of servo motor requires regulated supply voltage of *5V*. This consists of three wires namely signal, positive and ground wire.

It also comprises several internal parts which are the motor and gearbox, position sensor, an error amplifier, motor driver and a circuit to decode the requested position. Servo motor only rotates by the maximum of *180 degrees*.

4.1.3 The servo motor internal constitution

The servo motor used in this project is an assembly of four parts: an electrical DC motor, a gearbox, a position-sensing device which is usually a potentiometer and an electronic card to control and assess motor.

The servo motor body is composed of an electronic card receiving the reference signal to realize assessment. This card controls an electrical DC motor which will drive the pioneer through the speed-reducing gear as illustrated in the following Fig. 7.

The gearbox has two functions:

- Reducing the speed to provide an accurate tracking of relative position of the servo motor and to avoid damage of the system when movement is driven by its speed if it is very high.

- Increasing the torque by its mechanical movement of rotation. At an instant *t*, if we decrease the speed Ω leaving the same mechanical power P_{mec}, this will increase the torque *T*.

Fig. 8 shows a DC servo motor responses of rotating speed via supplying voltage $\Omega=f(U)$, electromagnetic torque via armature current $T=f(I_a)$ and torque via angular speed $T=f(\Omega)$.

Speed is related to supplying voltage and current is related to the electromagnetic torque. Hence for a given fixed speed, if our system must increase the mechanical power to move a heavier load (solar panel weight), this will increase current (knowing that *U* and Ω remain constant and electrical power $P_{el}=U.I$, must be equal to mechanical power $P_{mec}=T.\Omega$, when all internal losses are neglected). Since consumed energy by the system is generated by the panel itself, to improve efficiency, power consumption of the solar tracker is reduced since the servo motors supply the amount of torque just sufficient to move it (its mass is about *250 g*).

Fig. 8-a shows the angular speed Ω of the servo motor changed with the output voltage *U* of the drive unit. The speed Ω starts obviously at zero (servo motor at rest) to reach its maximal value *7.8 rad/s*. We observe that Ω increases in a linear manner with voltage *U* to stabilize at an approximate specific value for *5V*.

Fig. 8-b shows evolution of torque *T* via current *I*. The drive unit controls the output torque linearly, starting at $T_L= 16.3$ *kg cm*, to increase with current.

Fig. 8-c shows evolution of *T via* Ω. We notice that the servo motor keep its torque value even when its speed increases, but when the motor reaches its nominal speed of *7.7 rad/s*; servo motors supply the amount of torque *10 kg.cm* just sufficient to move it.

4.2 Servo motor working

PWM is used to control the motors. PWM analog signal will go through an electronic circuit and convert the analog signal into a digital signal. PWM in servos is used to control the direction and position of the motor. There were two servo motors used in this project for horizontal and vertical axis respectively.

Servo motors are controlled using an electrical cable composed of three wires to supply the motor (positive and ground) and the third one is used to transmit a PWM analog signal to control the motor positions. This means that it is the period of impulsions which determine the absolute angle of the output axis and then the position of the control shaft of servo motor. The signal is periodically repeated, in general every 20 milliseconds as shown in Fig. 9. This permits electronics to control and continuously correct the output axis angular position. This one is measured by the potentiometer. When the servo motor rotates, axis of servo motor changes the position that will modify the potentiometer resistance. The role of the electronic circuit is to control the motor so as output axis position will be conform to the received reference signal: it is an assessment.

5. Microcontroller and Programming

Our active sun tracker is controlled by PC program using an Arduino Uno. In this section, we will present the specifications of the microcontroller and the developed programming to conduct the exact system working.

5.1 The microcontroller

5.1.1 Advantages of the microcontroller

The use of microcontrollers for programming circuits posses various strong and real advantages. Actually, we find the spectacular evolution of IC (Integrated Circuit) design in recent years.

It encompasses various components decreasing the cumbersomeness of materials and IC, simplifying the tracing of printed circuits to drive data bus address, increasing system reliability and reducing cost.

5.1.2 Microcontroller role in a solar tracker system

The microcontroller converts analog signal captured from LDR to digital signal which will be compared to a tolerance input signal, to be transmitted to the servo motors in order to move the PV panels where it can receive maximum sunlight.

5.1.3 Microcontroller choice

Many designers propose microcontrollers (Microchip, Atmel, Texas-Instrument, Free Scale, NXP, Cypress, etc...). Each one proposes various families of microcontrollers (PIC and dpPIC from Microchip; AVR, AVR32 and ARM from Atmel, etc...). Each family contains tens of models, which are basically different by their memories sizes and the I/O pins number.

The choice of microcontroller is done on the basis of application even it is preferable to fix a family. Even if the PIC microcontroller of Microchip have contributed to popularise the architecture reduced instruction set computer (RISC), so much in the world of microcontrollers as well in the literature devoted to informatics architectures, there were not the only one circuits in the market. The microcontrollers of AVR family from Atmel, for which this paper have been dedicated, using this architecture and hence benefits various advantages.

The AVR family have a lot of advantages, cheap, low energy consumption, and a good support multi-platform. They are successful, given these specifications:

Good: they work well. They are easy to program in C++ language for the most basic functions. Adequate documentation exists.

Economic: A lot of pieces of 3–5 Euros, disposable from big distributors in small quantity.

Low energy consumption.

5.1.4 ATMEGA microcontroller

The microcontrollers of the family ATMEGA**,** in technology CMOS**,** are models of *8 bits* AVR based on architecture RISC. When we execute instructions in a simple clock cycle, the ATMEGA realises operations reaching *1 MIPS by MHZ* allowing simple systems design and low energy consumption**.**

5.1.5 Structure of an ATMEGA microcontroller

The ATMEGA328P microcontroller is featured by the following particularities:

- A Flash Memory of *32KB* for program storage.
- A SRAM Memory of *2KB* for variables storage.
- An EEPROM Memory *1KB* for permanent robot parameters storage.
- Technology RISC (one instruction per clock cycle) which confer a power of *20 million instructions per second* (MIPS) for a clock frequency of *20 MHz*.
- Include an UART (universal asynchronous receiver/transmitter**)** compatible RS232 for the communication with the PC.
- Include I2C Bus for the communication with the components I2C.
- An Analog/Digital converter ADC of *6 channels* of *10 bits*.
- Supplying voltage of *2.7 V* to *5.5 V*.

5.1.6 Synopsis

Fig. 10 shows the synopsis of the internal hardware architecture of the ATMEGA328P microcontroller:

5.1.7 Pins description

It is an IC of 28 pins dual in line shown in Fig. 11, where 14 are digital input/output of which 6 provide PWM outputs, 6 analog inputs, a 16MHz quartz crystal oscillator, an ICSP (In Circuit Serial Programming) header, an USB connection, a power jack and a reset button.

- VCC: supplying voltage (*+3V* to *+5V*).
- GND: ground.
- Port B (PB7... PB0): it is bidirectional I/O port of 8 bit with internal pull-up resistors chosen for each bit.
- PB6/XTAL1: External Oscillator amplifier input or free for internal clock.
- PB7/XTAL2: Output of the Oscillator amplifier.
- Port C (PC5 ... PC0): it is bidirectional I/O port of 7 bit with internal pull-up resistors selected for each bit.
- PC6/ RESET: Released by falling front maintained for more than *50ns* producing the reset of microcontroller, even if the clock is at rest.
- Port D (PD7 ... PD0): The D port is bidirectional I/O port of 8 bit with internal pull-up resistors chosen for each bit. It is used so as USART and inputs for external interruptions.
- AVcc: It is supplying voltage pin for the A/D converter which must be connected to *Vcc* via low pass filter to avoid parasites.
- AREF: It is the analog reference input for the A/D converter with a voltage of *2 V* to *AVcc* with low pass filter.

5.1.8 Oscillator

The external quartz crystal oscillator is connected on XTAL1, XTAL2 as shown in Fig. 12 to cadence the microcontroller. Crystal type Quartz frequency is from *4* to *16 MHZ* or ceramic resonator.

Using the external quartz oscillator, a capacitive damper of about *12* to *22 pF* must be connected as shown in Fig. 12 here up.

5.1.9 A/D Converter (ADC)

The Analog to Digital Converter integrated in the ATMEGA is doted of very interesting specifications with *10 bit* resolution, 6 simultaneous inputs. This ADC converts analog voltage to digital signal coded on *10 bit* described by resolution equation (2):

$$Resolution = \left(\frac{V_{in}}{V_{A.ref}} \times 1024 \right) - 1 \qquad (2)$$

5.2 Design of the solar tracker control circuit

A dual axis tracker based on four identical LDRs was constructed and tested to set the optimal values of the potentiometers R_{VIT} and R_{TOL} shown in both Fig. 3 and Fig. 13. The R_{TOL} tolerance was calculated in terms of the angle between the up side couple of (LDR1, LDR3) and down side couple of (LDR2, LDR4) sensors. After some initial and trial error testing, the optimal angle between these photo-resistors was evaluated experimentally to set the tolerance voltage value *TOL*. Precise results have been found because the system is working in close-loop system. This latter using photo sensors is the conventional control method of sun tracking systems. The photo sensors are used to discriminate the sun's position and then sending the proper analog electrical signals, converted to digital signal, proportional to controller error, which actuates the motors to track the sun [17], [28]. Circuit scheme of the designed system for horizontal and vertical axis is shown in Fig. 13. When the sun moves to the east or to the west, either the couple (LDR3, LDR4) or (LDR1, LDR2) will get more light, transforming the solar light intensity collected to electrical voltages $V_{LDR3,4}$ or $V_{LDR1,2}$ using the voltage dividers (Equ.1). These latter are sent to ADC ports (Pc_0, Pc_1) for the altitude angle or ports (Pc_2, Pc_3) for the azimuth angle tracking, to the microcontroller for comparison with the tolerance input signal *TOL* sent to ADC port (Pc_5), to control servo motors. These ones are acting the orientation of the PV panel towards the sun. Rotation directions for the azimuth and altitude angles tracking respectively the horizontal (H) and vertical (V) motors are controlled by using two differential amplifiers (op-amp-H, op-amp-V). Couples ($V_{LDR3,4}$, $V_{LDR1,2}$) and ($V_{LDR1,3}$, $V_{LDR2,4}$) voltages are sent to the microcontroller for average computation and comparison with *TOL*. According to the average differences between the voltages from LDR couples $d_{Vert} = |mean(V_{LDR1,3} - V_{LDR2,4})|$ or $d_{Horiz} = |mean(V_{LDR1,2} - V_{LDR3,4})|$are bigger or smaller than the fixed value *TOL*; the proper logic signals are sent to the errors op-amps to drive the DC motors. The width of PWM control signal shown in Fig. 9, generated by using AVR timers, determines the absolute angle of the output axis and then the position of the control shaft of servo motors**.** When the motors rotate, H and V axis change the positions that will accordingly modify the potentiometers resistances (position sensors of the assessment electronic card in Fig. 7) mounted on the shafts and provide the H and V feedback voltages. These ones will be compared to PWM control signals to determine the positions of the DC motors. Finally, H-motor and V-motor are turned in such directions clockwise (cw) or counter-clockwise (ccw) that the absolute values of d_{Horiz} and d_{Vert} become less than the *TOL* value and the motors are then stopped. When the light sensors have the same amount of resistance values (i.e. for the same rate of light), the error amplifiers give the same output (*0 V*) (i.e. the lunette in Fig. 5-c is pointed towards the sun) and since the potential difference at the motor terminals is zero, the panel does not rotate.

We have used the logic ISIS Proteus for the simulation of our montage in Fig.13. We present the assemblage of different parts of the system, before mentioned on the global electric scheme of the installation represented as follow:

We set the optimal value of potentiometer R_{VIT} depending on the weight of the PV panel. For our system we fixed R_{VIT} to *2.5 k*Ω.

If we choose a very small value of the tolerance, for example *TOL=0.0001V*; our panel will oscillate. The potentiometer R_{TOL} will be taken so that the difference is with a tolerance of *0.5V* for a proper working of our system.

5.3 Developing Environment

We have chosen the compiler gcc-avr which is compatible with most popular platforms (Windows, Linux and Mac).

To transmit the software PC program to the Atmega328p microcontroller, we must use conversion USB series module, it is the FTDI Basic Breakout in the same card comporting a microcontroller noted Arduino Uno.

Arduino Uno developing environment is a Java multi-Platform application, used as code editor and compiler, to transmit code to asynchronous serial liaison using C++ programming language.

The Atmega328P pin mapping with Arduino Uno board is shown in Fig. 14 for its programming using C++ language in Appendix A.

// **C++ Program compilation**

```
#include <Servo.h>   // include Servo library.  Include the class of Servo.h, allow for easily manipulating
                        the complete management of servo motor

Servo horizontal;     // horizontal servo. Create "initialize the object servo"
int servoh = 90;       // stand horizontal servo

Servo vertical;        // vertical servo
int servov = 90;       // stand vertical servo

// LDR pin connections
// name = analogpin;
int ldrlt = 0;    //LDR top left
int ldrrt = 1;    //LDR top rigt
int ldrld = 2;   //LDR down left
int ldrrd = 3;   // LDR down rigt


void setup()
{
  Serial.begin (9600);
// servo connections
// name.attacht(pin);
  horizontal.attach(9);
  vertical.attach(10);
}
void loop()
{
  int lt = analogRead(ldrlt);        // top left
  int rt = analogRead(ldrrt);       // top right
  int ld = analogRead(ldrld);       // down left
  int rd = analogRead(ldrrd);      // down right

  int dtime = analogRead(4)/20; // Read potentiometers
  int tol = analogRead(5)/4;

  int avt = (lt + rt) / 2;                 // Average value top
```

```
  int avd = (ld + rd) / 2;              // Average value down
  int avl = (lt + ld) / 2;              // Average value left
  int avr = (rt + rd) / 2;              // Average value right
  int dvert = avt - avd;                // Check the difference of up and down
  int dhoriz = avl - avr;               // Check the difference of left and right

  if (-1*tol > dvert || dvert > tol)   // Check if the difference is in the tolerance else change vertical angle
  {
  if (avt > avd)
  {
    servov = ++servov;
     if (servov > 180)
     {
      servov = 180;
     }
  }
  else if (avt < avd)
  {
    servov= --servov;
    if (servov < 0)
  {
    servov = 0;
  }
  }
  vertical.write(servov);
  }

  if (-1*tol >dhoriz ||dhoriz >tol)  //Check if the difference is in the tolerance else change horizontal angle
  {
  if (avl > avr)
  {
    servoh = --servoh;
    if (servoh < 0)
    {
    servoh = 0;
    }
  }
  else if (avl < avr)
  {
    servoh = ++servoh;
     if (servoh > 180)
     {
     servoh = 180;
     }
  }
  else if (avl = avr)
  {
    // nothing
  }
  horizontal.write(servoh);
  }
   delay(dtime);
}
```

Appendix A. Tracking control C++ Program.

6 Various steps of the mechanical design

In this section, we will design the mechanical parts adopted for the solar tracking mode working on the basis of horizontal and vertical directions of varying angle respectively from *0° to 180°* and from *0° to 90°*. The mechanical design consists of rotary joints and two DC servo motors.

6.1 Photovoltaic panel prototype

Fig. 15 shows our design as a prototype composed of wood plate. Its size is *460 × 285 mm* and its mass is about *250 g*. This woody plate will be fixed by seven vices in seven points on the vertical axis; three in front and four behind.

6.2 The lunette

Fig. 16 shows the lunette which is fixed to the photovoltaic panel prototype and placed on the same plan. It is composed of four LDR disposed in cross and optically isolated from each others, leading at a such way that the light intensity will not be identical only if the lunette is pointed towards the sun.

6.3 Vertical axis

Vertical axis is realized in wood of size *390 mm* each side. Dual ball bearing facilitates their rotation. Fig. 17 shows how we have fixed the servo motor HS-645MG standard deluxe in one side.

6.4 Horizontal axis

It is realized in such a way that ball bearing will be in the middle of the axis as shown in Fig. 18, in order to be able to drive the sole.

6.5. The basis

It is realized in wood of size *390×390 mm* as shown in Fig. 19. Its role is to insure the assize and the stability of the installation.

To orient the panel towards the solar rays, we must first of all, make the choice of the motors.

The size of the prototype tracker panel is imposed by the torques of servo motors. These constraints have conducted to the design of an experimental tracker where the quotations are mentioned on the Fig. 20 hereunder (*340mm×275mm*):

7 Management of system flowchart

The global program intended to a programmable circuit, is based on a well precise idea to satisfy the constructor catalogue and industrial context. This one is generally translated through a flowchart defining the various steps of the program.

7.1 Basic software design

The basic software flowchart of the solar tracker system is illustrated in Appendix. B as follow:

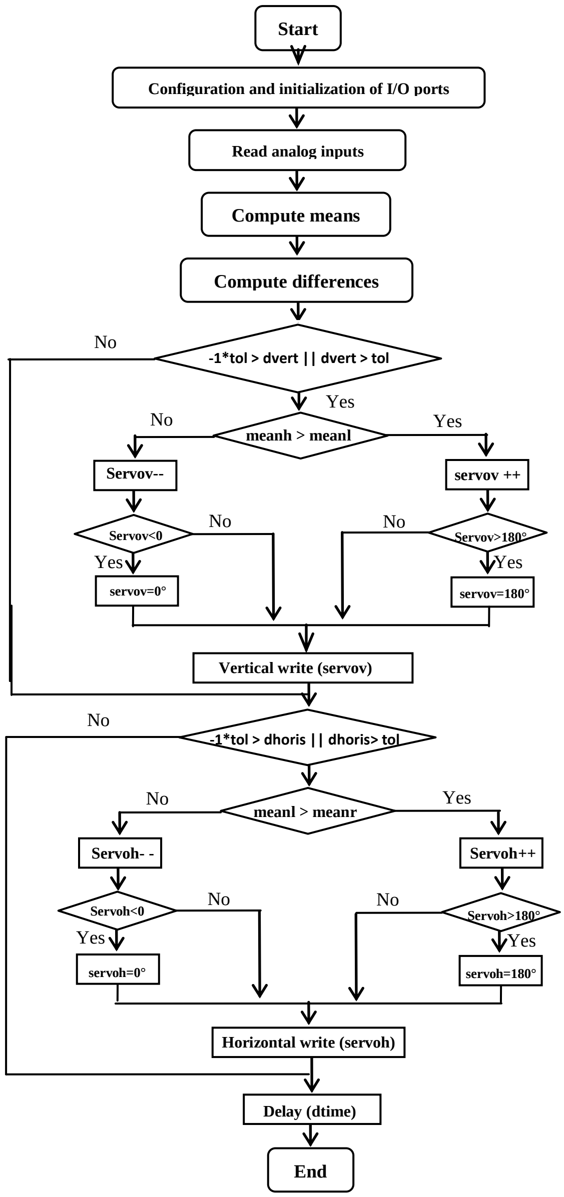

Appendix B. Tracking control flowchart.

7.2 Explanation of the flowchart

We begin by configuration and initialization of I/O ports.

It is the nomination of the type of configuration of inputs or outputs ports indicating the used pins.

LDRlt = 0; ➔ LDR top left

LDRrt = 1; ➔ LDR top right

LDRld = 2; ➔ LDR down left

LDRrd = 3; ➔ LDR down right

Initialize the object servo

servoh = 90 degrees; ➔ Stand horizontal servo

servov = 90 degrees; ➔ Stand vertical servo

to have the panel in its vertical position when supplying the system.

- *Read the analog inputs*

We acquire and convert the analog signal to digital the values captured by the sensors.

- *Compute the mean values (means)*

Compute the means values for each couple of LDR among the four sensors illustrated in Fig. 13, as follow:

Between LDR1 and LDR3 ➔ Mean value of the up side

Between LDR2 and LDR4 ➔ Mean value of the low side

Between LDR1 and LDR2 ➔ Mean value of the left side

Between LDR3 and LDR4 ➔ Mean value of the right side

- *Compute the difference values (Diffs)*

\- Compute the difference between the mean value of the up and low sides, to control the vertical motor.

\- Compute the difference between the mean value of the left and right sides, to control the horizontal motor.

- *-1*tol > dvert || dvert > tol*

The previous obtained result « Compute diffs » will be compared to TOLERANCE input signal (tol.). If we obtain an equal value, the motor is at rest; otherwise if we have a different value the motor will move to change vertical angle.

- *meanh > meanl ; (h :high ; l :low)*

It will be the values of the vertical which permit to correct the vertical system position. The motor will move the panel toward the side where there is a big value, but when reached angle is 180° or 0°, the motor stops.

- *-1*tol > dhoriz || dhoriz > tol*

The previous obtained result « Compute diffs » will be compared to TOLERANCE input signal (tol.). If we obtain an equal value, the motor is at rest; otherwise if we have a different value the motor will move to change horizontal angle.

- *meanl> meanr ; (l :left ; r :right)*

It will be the values of the horizontal which permit to correct the horizontal system position. The motor will move the panel toward the side where there is a big value, but when reached angle is 180° or 0°, the motor stops.

Two delay times: short and long pauses.

The short pause is the delay of the position of the PV Panel relatively to the sun ray. We can fix a delay of 30 minutes to avoid wasting of energy, after which the panel change of inclination of 9 or 10 degrees following the new position of the sun.

The long mean pause of 12 h (from 10h to 15h depending on the season) will be at the end of the day, which permits to panels to have their initial positions.

8 Conclusion

The described program has satisfied the control conditions for the good working of the system so as results are encouraging. In fact, the program repartition permits to distinguish various realized operations. Instruction commented of the program guides in the methodical repairing of the functions. It facilitates the modifications which could be made during these works. The proposed montage uses a limited number of components, easy to use and occupy a restricted space which could be integrated in a complete photovoltaic system. The total cost reached only 150 Euros, and the period of realization is about 40 days. It has an effective contribution on the environment and could be improved. Two degrees of freedom orientation is made able to truck the sun position. In our case, we have tested the system using the flash-light of a moving electrical lamp to shine it at the sensors; the tracker has been following it around, which was successful verifying its efficient and correct working. The microcontroller is used to control exact shaft position of DC servo motors which ensure point to point intermittent stable movement. The microcontroller is designed to rotate the panel from 0 to 180 degrees. The presented dual axis solar panel tracking system keeps the solar photovoltaic panel perpendicular to the sun throughout the year to improve the efficiency of the system.

As advancements in photovoltaic trackers technologies have decreased investment prices, this project could be extended to power supply isolated villages or farms by mounting more optimal large and scheduled moving panels providing a huge solar energy. Scheduled tracking must use a computer program to change the angle of the panel based on date, time, and its physical location even under cloud coverage.

References

[1] Finster C. "University Santa Maria Heliostat (El heliostato de la Universidad Santa Maria)", Scientia, **119**, pp.5–20, (1962).

[2] Saavedra AS. "Design of a sun tracking mechanism for automatic measurement of direct solar radiation (Diseno de un servomecanismo seguidor solar para un instrumento registrador de la irradiacio´n solar directa)", Memoria, Technical University Federico Santa Maria, Valparaiso, Chile, (1963).

[3] Abdallah S., Nijmeh S. "Two axes sun tracking system with PLC control", *Energy Conversion and Management*, **45**(11-12), pp.1931-1939, (2004).

[4] Roth P., Georgiev A., Boudinov H. "Cheap two-axis sun following device", *Energy conversion and Management*, **46**(7-8), pp.1179-1192, (2005).

[5] Yazidi A., Betin F., Notton G. And Capolino G. A. "Low cost two-axis solar tracker with high precision positioning", *Proceedings of the International Symposiumon Environment, Identities & Mediterranean Area ISEIM'2006,* Corte-Ajaccio, France, pp.211–216, July (2006).

[6] Rustemli S., Dincadam F., Demirtas M. “Performance comparison of the sun tracking system and fixed system in the application of heating and lighting”, *Arabian J Sci Eng*, **35**(2B), pp.171–183, (2010).

[7] Eke R., Senturk A. “Performance comparison of a double-axis sun tracking versus fixed PV system”, *Solar Energy*, **86**(9), pp.2665–2672, (2012).

[8] Lazaroiu G.C., Longo M., Roscia M., Pagano M. “Comparative analysis of fixed and sun tracking low power PV systems considering energy consumption”, *Energy Conversion and Management*, **92**, pp.143–148, (2015).

[9] Tian-Pau Chang “Output energy of a photovoltaic module mounted on a single axis tracking system”, *Applied Energy*, **86**(10), pp.2071–2078, (2009).

[10] Sefa I., Demirtas M., Çolak I. “Application of one-axis sun tracking system”, *Energy Conversion and Management*, **50**(11), pp.2709–2718, (2009).

[11] Ponniran A., Hashim A., Joret A. “A Design of Low Power Single Axis Solar Tracking System Regardless of Motor Speed”, *Internal Journal of Intergrated Engineering*, **3**(2), pp.5–9, (2011).

[12] Huang B.J., Ding WL, Huang YC. “Long-term field test of solar power generation using one axis 3-position sun tracker”, *Solar Energy*, **85**(9), pp.1935–1944, (2011).

[13] Seme S., Stemberger G., Vorsic J. “Maximum efficiency trajectories of a two axis sun tracking system determined considering system consumption”, *IEEE Trans Power Electron*, **26**(4), pp.1280–1290, (2011).

[14] Koussa M., Cheknane A., Hadji S., Haddadi M., Noureddine S. “Measured and modelled improvement in solar energy yield from flat plate photovoltaic systems utilizing different tracking systems and under a range of environmental conditions”, *Applied Energy*, **88**(5), pp.1756–1771, (2011).

[15] Saravanan C., Panneerselvam Dr. M.A., William Christopher I. “A Novel Low Cost Automatic Solar Tracking System”, *International Journal of Computer Applications*, **31(**9), pp.0975–8887, October (2011).

[16] Mousazadeh H., Keyhani A., Javadi A., Mobli H., Abrinia K., Sharifi A.“A review of principle and sun-tracking methods for maximizing solar systems output”, *Review Sustain Energy Ren*, **13**(8), pp.1800-1818, (2009).

[17] Yilmaz S., Ozcalik H. R., Dogmus 0., Dincer F., Akgol O., Karaaslan M. “Design of two axes sun tracking controller with analytically solar radiation calculation”, *Renewable and Sustainable Energy Review*, **43**, pp.997–1005, (2015).

[18] Yao Y., Hu Y., Gao S., Yang G., Du J. "A multipurpose dual-axis solar tracker with two tracking strategies", *Renewable Energy*, **72**, pp.88-98, (2014).

[19] Nakano Y. "Ultra-High Efficiency Photovoltaic Cells for Large Scale Solar Power Generation", *Ambio*, **41**(2), pp. 125-131, (2012).

[20] Ghaedi A., Abbaspour A., Fotuhi-Friuzabad M., Parvania M. "Incorporating Large Photovoltaic Farms in Power Generation System Adequacy Assessment," *Transactions on Electrical Engineering*, *Scientia Iranica*, **21**(3), pp. 924–934, (2014).

[21] Zerhouni FZ., Zerhouni MH., Zegrar M. "Modelling Polycristallin Photovoltaic Cells Using Design of Experiments," *Transactions on Electrical Engineering*, *Scientia Iranica*, **21**(6), pp. 2273–2279, (2014).

[22] Dattaa A., Bhattacharyab G., Mukherjeec D., Sahad H. "An efficient technique for controlling power flow in a single stage grid-connected photovoltaic system," *Transactions on Electrical Engineering*, *Scientia Iranica*, **21**(3), pp.885–897, (2014).

[23] Yaiche M.R., Bouhanik A., Bekkouche S.M.A., Malek A., Benouaz T. "Revised solar maps of Algeria based on sunshine duration," *Energy Conversion and Management*, **82**, pp.114-123, (2014).

[24] Stambouli A. B. "Promotion of renewable energies in Algeria: Strategies and perspectives," *Renewable and Sustainable Energy Reviews*, **15**(2), pp.1169-1181, (2011).

[25] Adouane M., Haddadi M., Touafek K., Aitcheikh S. "Monitoring and smart management for hybrid plants (photovoltaic-generator) in Ghardaia," *Journal of Renewable and Sustainable Energy*, **6**(2), (2014).

[26] Yacef R., Mellit A., Belaid S., Sen Z. "New combined models for estimating daily global solar radiation from measured air temperature in semi-arid climates: application in Ghardaia, Algeria," *Energy Conversion and Management*, **79**, pp.606-615, (2014).

[27]] Behar O., Khellaf A., Mohammedi K. "Comparison of solar radiation models and their validation under Algerian climate – The case of direct irradiance", *Energy Conversion and Management*, **98**, pp.236–251, (2015).

[28] Bentaher H., Kaich H., Ayadi N., Ben Hmouda M., Maalej A., Lemmer U. "A simple tracking system to monitor solar PV panels", *Energy Conversion and Management*, **78**, pp.872– 875, (2014).

Abdelhamid Mansouri was born in Sidi-Okba, Algeria, in 1951. He received the D.E.S. (Diploma of Higher Studies) degree from the University of Algiers, in 1979 and the M.Phil. degree in Electrical Engineering from the University of Sétif in 1996. He was an assistant lecturer in the Department of Physics, University of Annaba in 1979. He was Electrical Engineer in Industrial Societies ENAGEO & ELATEX from 1981 to 1983. Currently, he is a Lecturer in the Department of Electrical Engineering, University of Sétif-1, where he has been since 1983. Member of laboratory of power electronics and industrial control (LEPCI), his research interests are in the area of identification and optimal control of electrical machines, artificial intelligence techniques and renewable energies.

Fateh Krim received B.Sc. degree from Claude Bernard University of Lyon, France, in 1976, M. Sc and Engineer degrees in electrical engineering from Ecole Centrale , Lyon, in 1979, the Ph D from Polytechnic National Institute of Grenoble, France , and the special doctorate from University of Sétif, Algeria, in 1982 and 1996 respectively. From 1982 to 1985, he was head of IC design department at CIT-Alcatel, Paris, France. He is currently a professor of electrical engineering at University of Sétif-1, Algeria and Director of laboratory of power electronics and industrial electronics. His main research interests are systems control, power and industrial electronics, renewable energies. In these fields, he has more than 80 papers in international journals and refereed conference proceedings. He is reviewer in 13 journals. **Professor Fateh Krim** is a senior IEEE Member and member of IEEE Industrial Electronics Society, IEEE Power Electronics Society, IEEE Power Engineering Society, and IEEE Computational Intelligence Society. He is president of IEEE Algeria Section and Industrial electronics and Industry applications chapter.

Zakaria Khouni was born in Sétif, Algeria, in 1988. He received his Bachelor degree in Electrical Engineering (EEA) and his master's degree in Industrial Electronics from Ferhat Abbas Sétif-1 University, Sétif, Algeria, in 2012 and 2014, respectively. He is currently pursuing his Ph.D. in Electronics Department at Sétif-1 University's, LCCNS Laboratory. His research interests include embedded system technologies, Fuzzy logic systems, DSP system and FPGA cards.

List of captions

Table 1. Solar potential in Algeria.

Figure 1. Classes of dual axis solar trackers.

Figure 2. Efficiency comparisons of fixed support design and tracker panels.

Figure 3. Block diagram of the overall system.

Figure 4. Voltage regulator.

Figure 5-a. Cds LDR.

Figure 5-b. LDR characteristics.

Figure 5-c. Lunette composed of four LDR.

Figure 6. Servo motor blocks.

Figure 7. Different parts of the servo motor.

Figure 8-a. Motor speed $\Omega = f(U)$.

Figure 8-b. Torque $T = f(I)$.

Figure 8-c. Torque $T = f(\Omega)$.

Figure 9. Position of the pioneer relatively to PWM signal.

Figure 10. Synopsis of the ATMEGA328P.

Figure 11. ATMEGA328 typical pins.

Figure 12. Oscillator circuit.

Figure 13. Solar tracker control circuit.

Figure 14. Atmega328P pin mapping with Arduino Uno board.

Appendix A. Tracking control C++ Program.

Figure 15. Photovoltaic panel prototype.

Figure 16. Lunette of the tracker.

Figure 17. Vertical axis of the tracker.

Figure 18. Horizontal axis of the tracker.

Figure 19. Tracker basis.

Figure 20. Prototype of the tracker panel.

Appendix B. Tracking control flowchart.

List of tables

Table 1.

zone	Coast zone	High planes zone	Sahara
Surface area (%)	4	10	86
Sunny mean period (hours/annum)	2650	3000	3500
Mean energy received (KWh/m^2/annum)	1700	1900	2650

List of figures

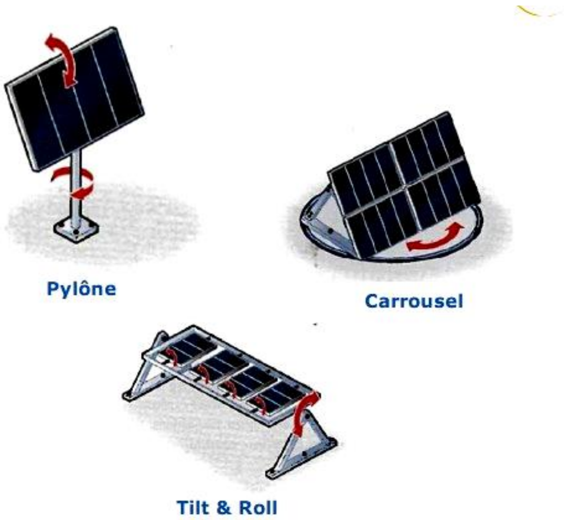

Figure 1.

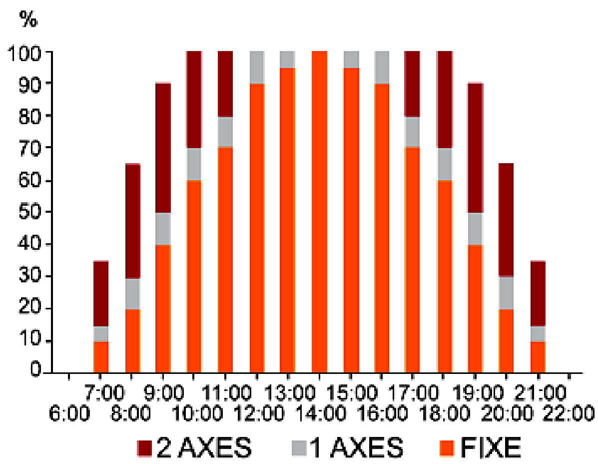

Figure 2.

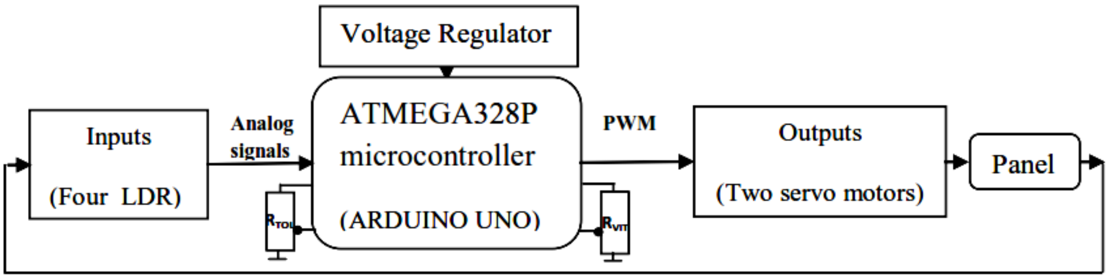

Figure 3.

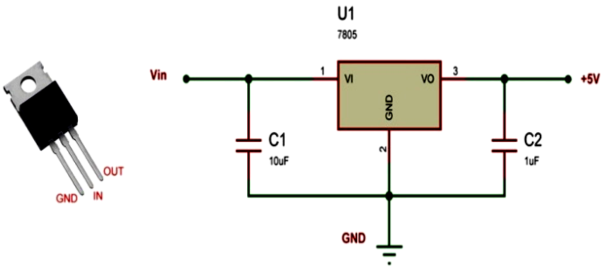

Figure 4.

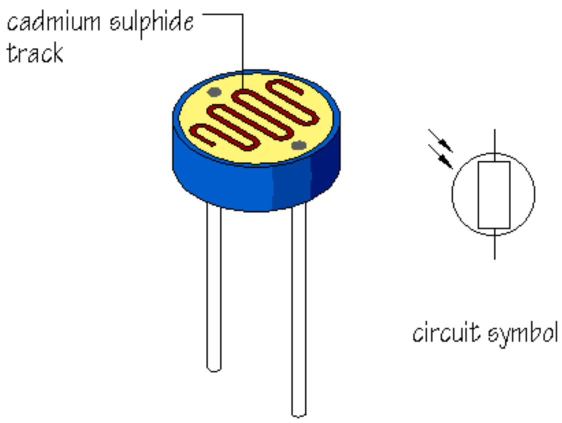

Figure 5-a.

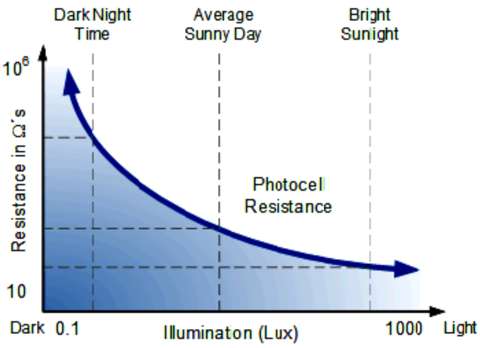

Figure 5-b.

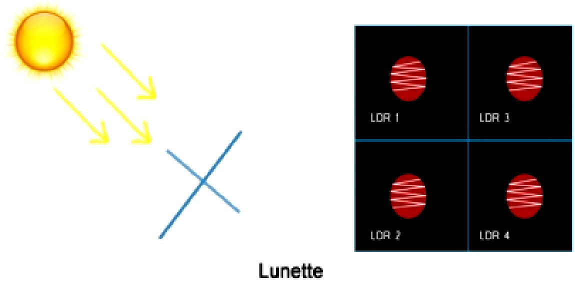

Figure 5-c.

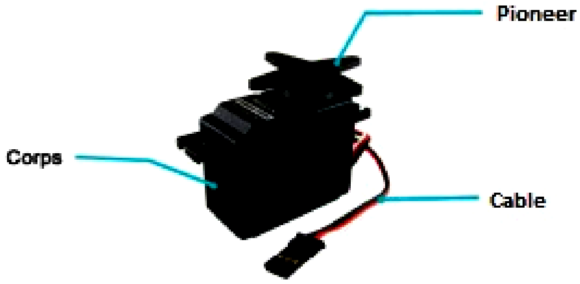

Figure 6.

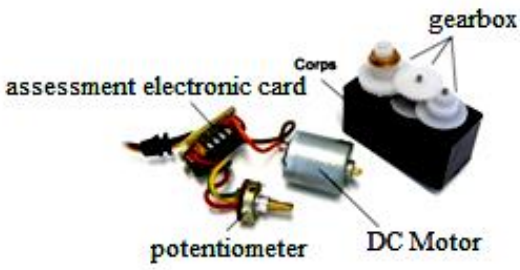

Figure 7.

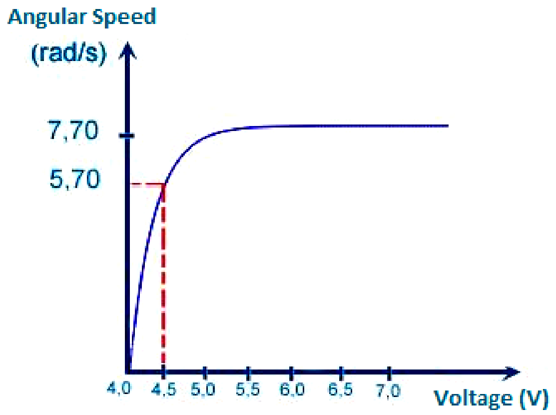

Figure 8-a.

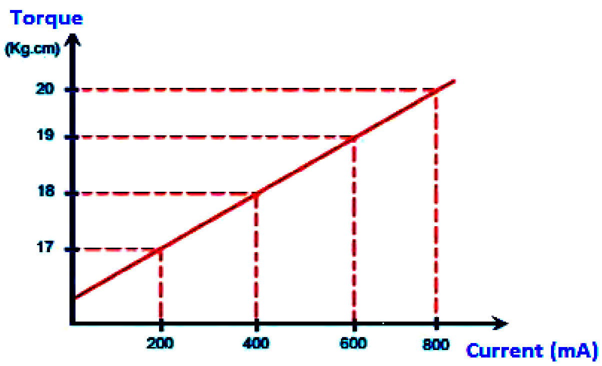

Figure 8-b.

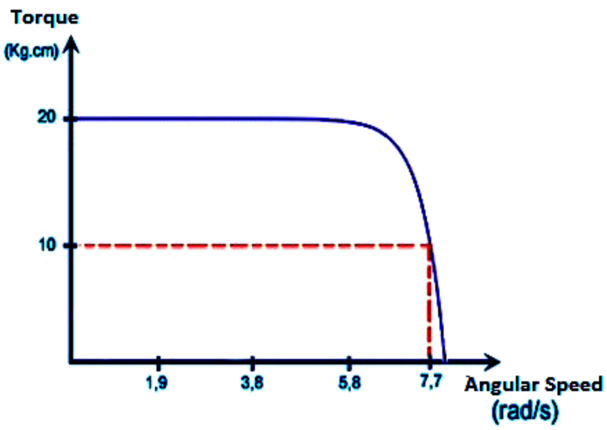

Figure 8-c.

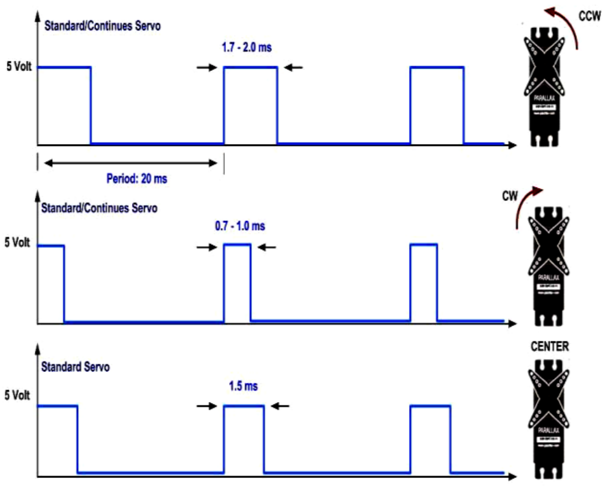

Servo Motor PWM Timing Diagram

Figure 9.

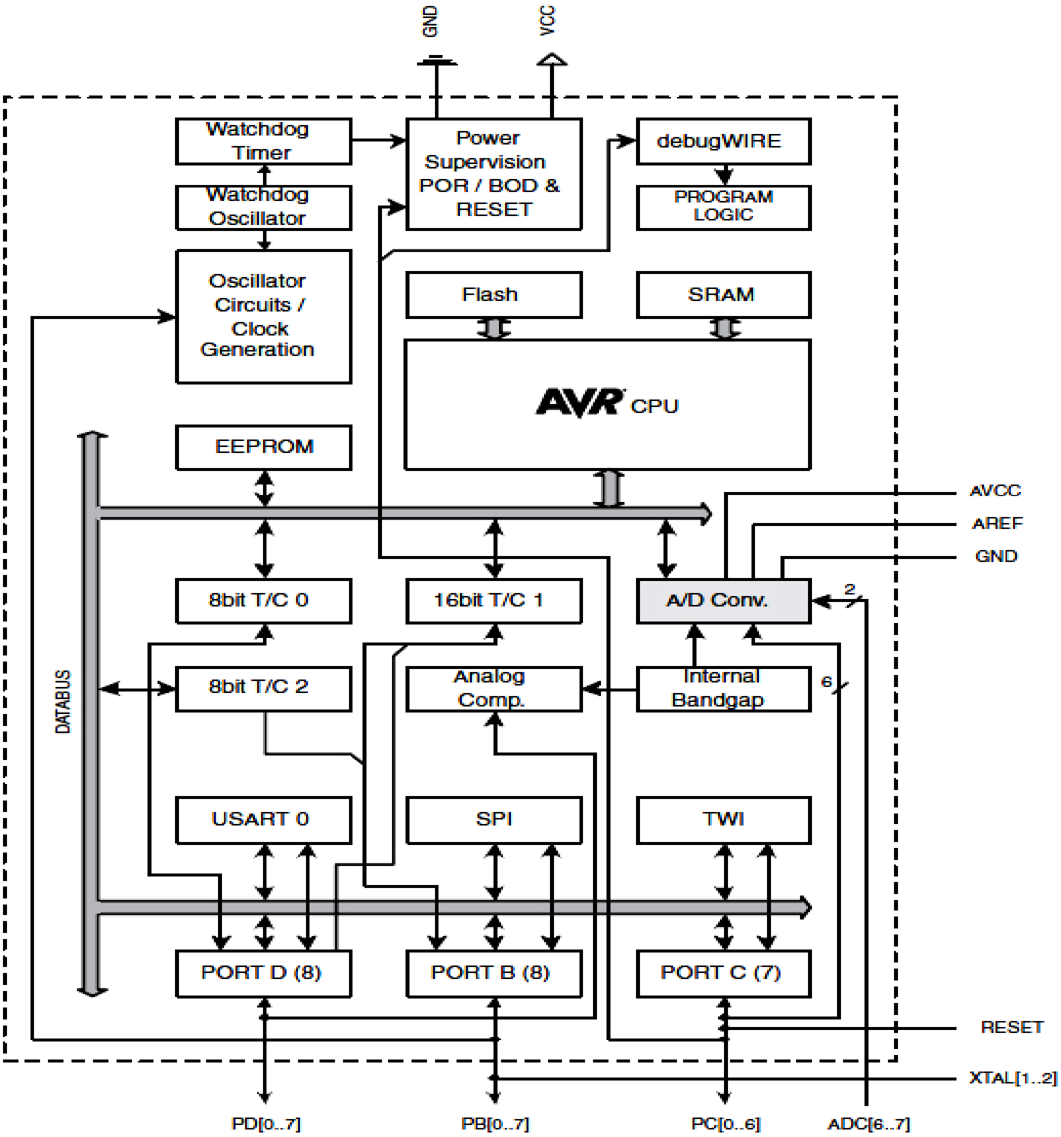
GND
VCC
Watchdog Timer
Watchdog Oscillator
Oscillator Circuits / Clock Generation
Power Supervision POR / BOD & RESET
debugWIRE
PROGRAM LOGIC
Flash
SRAM
AVR CPU
EEPROM
DATABUS
AVCC
AREF
GND
8bit T/C 0
16bit T/C 1
A/D Conv.
2
8bit T/C 2
Analog Comp.
Internal Bandgap
6
USART 0
SPI
TWI
PORT D (8)
PORT B (8)
PORT C (7)
RESET
XTAL[1..2]
PD[0..7]
PB[0..7]
PC[0..6]
ADC[6..7]

Figure 10.

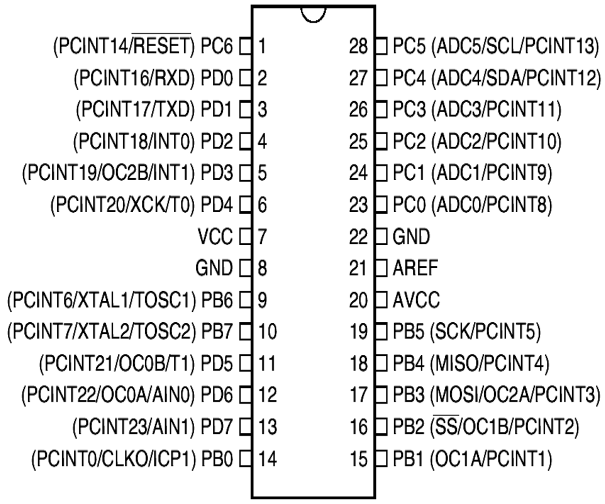

Figure 11.

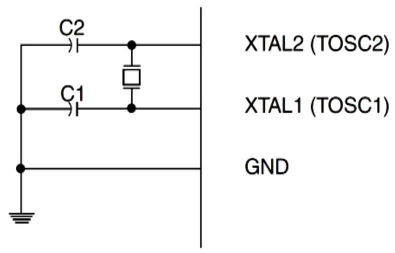

Figure 12.

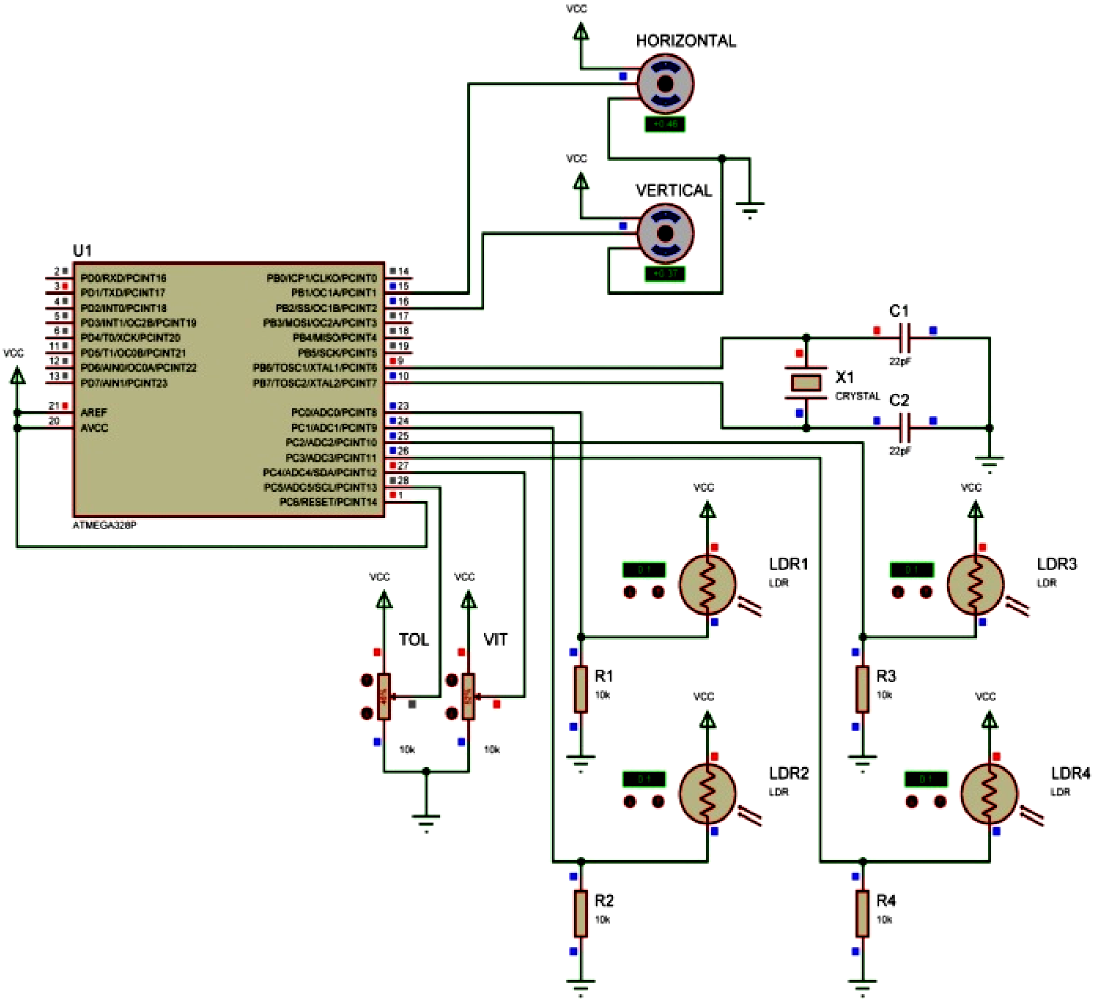
VCC
HORIZONTAL
VERTICAL
U1
PD0/RXD/PCINT16
PD1/TXD/PCINT17
PD2/INT0/PCINT18
PD3/INT1/OC2B/PCINT19
PD4/T0/XCK/PCINT20
PD5/T1/OC0B/PCINT21
PD6/AIN0/OC0A/PCINT22
PD7/AIN1/PCINT23
AREF
AVCC
PB0/ICP1/CLKO/PCINT0
PB1/OC1A/PCINT1
PB2/SS/OC1B/PCINT2
PB3/MOSI/OC2A/PCINT3
PB4/MISO/PCINT4
PB5/SCK/PCINT5
PB6/TOSC1/XTAL1/PCINT6
PB7/TOSC2/XTAL2/PCINT7
PC0/ADC0/PCINT8
PC1/ADC1/PCINT9
PC2/ADC2/PCINT10
PC3/ADC3/PCINT11
PC4/ADC4/SDA/PCINT12
PC5/ADC5/SCL/PCINT13
PC6/RESET/PCINT14
ATMEGA328P
C1
22pF
X1
CRYSTAL
C2
22pF
LDR1
LDR
LDR3
LDR
LDR2
LDR
LDR4
LDR
R1
10k
R3
10k
R2
10k
R4
10k
TOL
VIT
10k
10k

Figure 13.

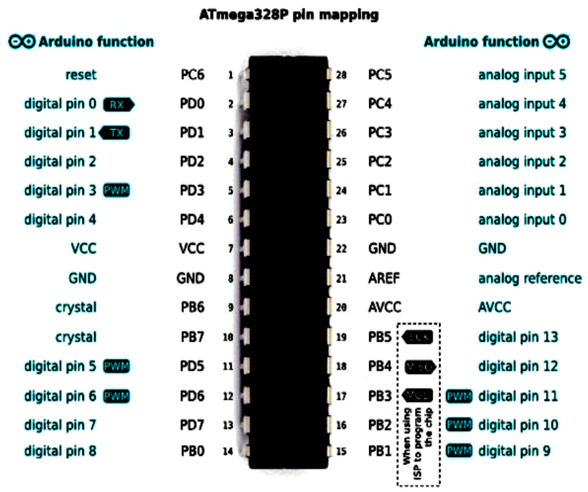

Figure 14.

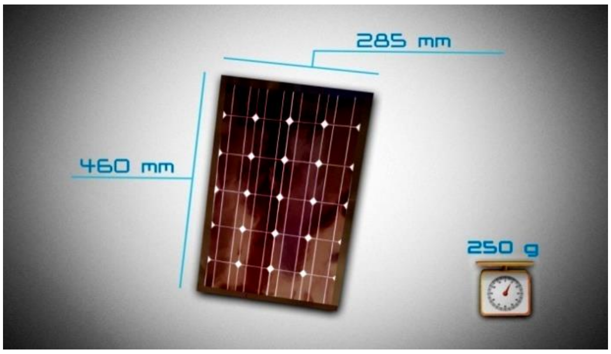

Figure 15.

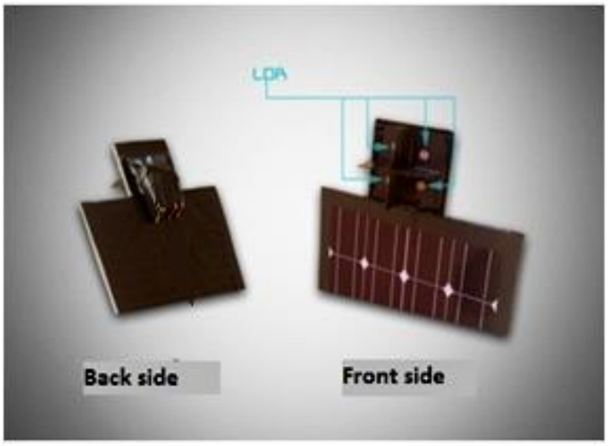

Figure 16.

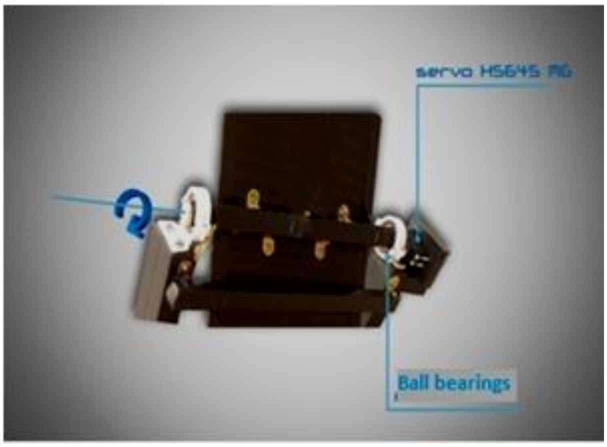

Figure 17.

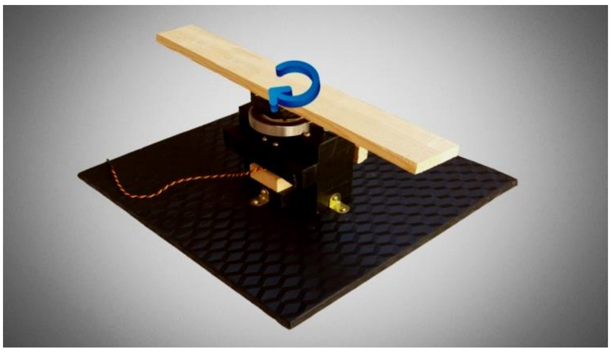

Figure 18.

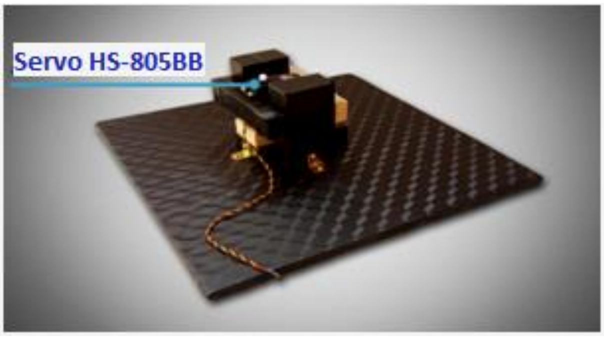

Figure 19.

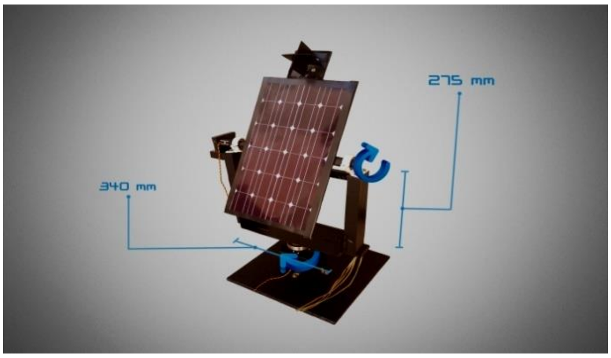

Figure 20.